

## Spatial separation of different drug substances in one microneedle array patch by combining inkjet printing and micromolding technology

Lukas C. Lammerding, Awadhi Arora, Sebastian Braun, Jörg Breitzkreutz

Article - Version of Record



### Suggested Citation:

Lammerding, L., Arora, A., Braun, S., & Breitzkreutz, J. (2024). Spatial separation of different drug substances in one microneedle array patch by combining inkjet printing and micromolding technology. *International Journal of Pharmaceutics*, 670, Article 125102. <https://doi.org/10.1016/j.ijpharm.2024.125102>

Wissen, wo das Wissen ist.



UNIVERSITÄTS- UND  
LANDESBIBLIOTHEK  
DÜSSELDORF

This version is available at:

URN: <https://nbn-resolving.org/urn:nbn:de:hbz:061-20250109-132156-2>

Terms of Use:

This work is licensed under the Creative Commons Attribution 4.0 International License.

For more information see: <https://creativecommons.org/licenses/by/4.0>



# Spatial separation of different drug substances in one microneedle array patch by combining inkjet printing and micromolding technology

Lukas C. Lammerding, Awadhi Arora, Sebastian Braun, Jörg Breitzkreutz\*

Heinrich Heine University Duesseldorf, Faculty of Mathematics and Natural Sciences, Institute of Pharmaceutics and Biopharmaceutics, Universitätsstraße 1, Duesseldorf 40225, Germany

## ARTICLE INFO

### Keywords:

Transdermal drug delivery  
Inkjet printing  
Microneedle array patches  
Micromolding  
Personalized medicine

## ABSTRACT

Transdermal drug delivery using microneedle array patches has been investigated using a wide range of drug substances. Inkjet printing and micromolding are established methods for the production of microneedle array patches and both were used to combine lisinopril embedded in povidone and ibuprofen in Eudragit® RS / RL in a single patch. Dissolution studies, visual inspection, mechanical strength and insertion into an artificial skin membrane model were investigated. A clear spatial separation of the polymers / drugs was observed. Microneedle array patches containing povidone and Eudragit® RS / RL showed a height reduction below 10 %. 97.14 ± 3.76 % of the microneedles made of povidone and Eudragit® RS and 97.50 ± 2.13 % made of povidone and Eudragit® RL pierced the second layer of Parafilm® M. This indicated a sufficient insertion into the membrane model. 132.14 ± 47.47 µg (Eudragit® RS) and 135.02 ± 3.34 µg (Eudragit® RL) lisinopril has been dissolved after 9 min. It was possible to vary the dissolution of ibuprofen using both types of Eudragit®. 211.80 ± 22.98 µg ibuprofen were dissolved after 24 h (Eudragit® RS) and 445.16 ± 9.98 µg after 6 h (Eudragit® RL). The microneedles successfully pierced human skin and both drug substances permeated across it. This could lead to an interesting approach to combining incompatible drugs in one patch.

## 1. Introduction

Transdermal drug delivery systems (TDS) offer the possibility to administer active pharmaceutical ingredients (APIs) bypassing the gastrointestinal tract (Alkilani et al., 2015). TDS may reduce side effects compared to oral drug delivery and reduce drug level fluctuations (Ma and Wu, 2017). However, the number of APIs used for transdermal drug delivery is highly limited due to the barrier function of the stratum corneum (SC) of the human skin (Scheuplein and Blank, 1971). Microneedle array patches (MAPs) may overcome this problem. MAPs consist of micrometer-sized needles (usually in the range between 100 and 1000 µm) attached to a coherent baseplate (Kang et al., 2021). MAPs are strong and sharp enough to pierce the SC and hence overcome the barrier function. The enhancement of transdermal drug delivery using MAPs has been described for small molecule APIs (Luo et al., 2019) as well as for peptides and vaccines (Pires et al., 2020). Transdermal delivery is advantageous compared to peroral delivery of proteins because of the acidic conditions and the enzymatic activities of the stomach enforcing the degradation of the proteins (Wiechers, 1989). Furthermore, MAPs are too short to reach nerve fibers enabling painless

administration (Kaushik et al., 2001). This may increase the adherence in patients with needle aversion in contrast to subcutaneous or intramuscular injections. Different types of MAPs are described in literature. Solid microneedles often consist of stainless steel and do not contain any API (Verbaan et al., 2007). The steel needles pierce the SC and e.g. an API-containing solution is applied to the damaged skin (Martanto et al., 2004). Coated microneedles are solid microneedles coated with an API-containing film. After piercing the skin the coating dissolves and enables transdermal drug delivery. Even the application of coated microneedles to the eye has been described (Jiang et al., 2007). Hollow microneedles form a pore or tunnel after piercing the SC and enable diffusion of APIs through the pore. Hollow microneedles contain the APIs loaded as a powder (Carcamo-Martinez et al., 2021) or as a solution (Wang et al., 2006). Dissolvable microneedles usually consist of a water-soluble polymer. The polymers dissolve after piercing the SC and enable drug delivery of an incorporated API. Dissolving microneedles were manufactured from different polymers like hyaluronic acid (Maurya et al., 2018; Panda et al., 2021), polyvinyl alcohol in combination with povidone (Peng et al., 2021) and hydroxypropyl methylcellulose (Aung et al., 2019). However, the most commonly used polymer for the

\* Corresponding author.

E-mail address: [joerg.breitzkreutz@hhu.de](mailto:joerg.breitzkreutz@hhu.de) (J. Breitzkreutz).

<https://doi.org/10.1016/j.ijpharm.2024.125102>

Received 9 September 2024; Received in revised form 16 December 2024; Accepted 17 December 2024

Available online 19 December 2024

0378-5173/© 2024 The Authors. Published by Elsevier B.V. This is an open access article under the CC BY license (<http://creativecommons.org/licenses/by/4.0/>).

manufacturing of dissolvable microneedles is povidone. The successful transdermal delivery has been described using APIs as nanosuspensions (Altuntas et al., 2022; Rojekar et al., 2021), dissolved in the polymer (Xing et al., 2021) or as a nanoemulsion (Nasiri et al., 2022). Another subtype of dissolvable MAPs are biodegradable MAPs for extended-release drug delivery. Usually, poly(lactic-co-glycolic acid) (PLGA) is used (Nguyen and Banga, 2018). Separable MAPs consist of a baseplate that is separable from the needle tips (Chu and Prausnitz, 2011). The tips remain in the skin after piercing the SC and the baseplate is removed. Hydrogel forming or swellable MAPs are made of a polymer that swells in the skin (Zhao et al., 2023) and offer the possibility for extended-release drug delivery.

Mechanical properties of the microneedles and the shape of the needles have a big impact on the potential of drug delivery (Bal et al., 2010). Different shapes like pyramidal (Lau et al., 2017), obelisk-type (Kim et al., 2018) and bullet-type (Seong et al., 2017) needles were investigated. Different modifications of dissolvable microneedles are possible to vary the dissolution profile of APIs. It is possible to manufacture extended-release microneedles by increasing the molecular weight of the dissolvable polymers (Kathuria et al., 2020) and by using biodegradable polymers like PLGA (Paredes et al., 2021) or polylactic acid (Palakurthi et al., 2011). Another option is the use of slowly dissolving polymers like aminoalkyl methacrylate copolymer E (Eudragit® E) (Matadh et al., 2022) or the use of extended-release polymers known from tableting (Aung et al., 2023).

Different methods for the production of dissolvable MAPs are described. The most commonly used manufacturing technique is called micromolding. A micromold made of silicon serves as a negative. Micrometer-sized cavities are filled with a polymer-containing solution using overpressure (Volpe-Zanutto et al., 2021) or centrifugation (Lee et al., 2008). Furthermore, inkjet printing offers the possibility to precisely fill single cavities of the micromold (Lammerding and Breitzkreutz, 2023) and reduce the waste of API during the manufacturing of MAPs. Inkjet printing is a technique generating droplets in the picoliter size (Liu and Derby, 2019). It can be distinguished between continuous inkjet printing (CIJ) (Martin et al., 2008) and drop-on-demand inkjet printing (DoD) (Singh et al., 2010). DoD using a piezo-electric actuator leads to very precise printing results because it is possible to deposit one droplet per pixel. Inkjet printing is an established method for preparation of personalized medicines. Orodispersible films containing water-soluble APIs (Thabet et al., 2018) were investigated as well as porous substrates containing water-insoluble APIs (Cheow et al., 2015). It has been described that inkjet printing is a suitable tool for the manufacturing of vaccine-containing microneedles (Allen et al., 2016) and even the precise manufacturing of multilayer MAPs (Lammerding et al., 2023) is possible. However, inkjet printing is still limited to povidone as a rapidly dissolving polymer. The viscosity of the ink formulation must not be too high. Other studies showed a new printing method for the manufacturing of dissolvable MAPs using ink formulations of high viscosities (Vander Straeten et al., 2024). Another approach is the manufacturing of MAPs using electrohydrodynamic coating of microparticles onto MAPs (Angkawitwong et al., 2020).

Aim of this study was to investigate the feasibility to combine different APIs incorporated in different polymers in one MAP. Different APIs have been combined in one patch before (Quinn et al., 2015). However, all needles were of the same composition. Every microneedle was loaded with all APIs. This could be problematic when incorporating two or more incompatible APIs in one MAP. A povidone-containing ink loaded with lisinopril as a peptidomimetic drug has been used to prepare a rapidly dissolving part of the needles. After that, the other cavities have been filled with an extended-release polymer loaded with ibuprofen as a model API using a centrifugation method. Ethyl cellulose and Eudragit® RS and RL were selected as the extended-release polymers. These polymers were already used for the production of MAPs or other dosage forms (Aung et al., 2023). Ethyl cellulose is known for its biocompatibility in combination with macrogol as a pore forming agent

(Frohoff-Hulsmann et al., 1999). Different methods have been investigated to verify a successful spatial separation of the polymers and of the APIs, respectively. The combination of inkjet printing and micromolding could be an interesting approach to combine incompatible APIs in one MAP widening the applicability for personalized medicine.

## 2. Material and methods

### 2.1. Material

Lisinopril dihydrate was purchased from Zhejiang Huahai Pharmaceutical (Zhejiang, China). Ibuprofen was obtained from Caesar & Loretz (Hilden, Germany). Ammonium methacrylate type A and B (Eudragit® RL PO and Eudragit® RS PO) were kindly provided by Evonik Industries (Essen, Germany). Ethyl cellulose was obtained from Ashland (Düsseldorf, Germany). Polyethylene glycol 400 (Macrogol 400, PEG 400), polysorbate 20 (Tween® 20) and glycerol 85 % were purchased from Caesar & Loretz (Hilden, Germany). Polyvinylpyrrolidone (Povidone, PVP) was kindly provided from BASF (Kollidon® K17, Ludwigshafen, Germany). Ethyl acetate was bought from Fisher Scientific (Geel, Belgium). Acetonitrile in high performance liquid chromatography grade was purchased from Carlo Erba Reagents (Cal-de-Reuil, France). Sodium chloride and phosphoric acid 85 % were bought from Sigma-Aldrich (St. Louis, Missouri, USA). Potassium chloride was obtained from VWR (Darmstadt, Germany). Disodium hydrogen phosphate was purchased from Carl Roth (Karlsruhe, Germany), potassium dihydrogen phosphate from Chemsolute (Renningen, Germany) and sodium dihydrogen phosphate from Merck (Darmstadt, Germany). Demineralized water was used as a solvent and ultra-purified water using a Milli-Q® apparatus (Merck, Darmstadt, Germany) for high performance liquid chromatography. Silicone molds for the manufacturing of microneedle array patches were kindly provided by LTS Lohmann-Therapiesysteme (Andernach, Germany). Every mold contained 300 cavities (pyramidal-shaped, 300 x 300 µm base area and 650 µm height). The cavities had an interspacing of 0.5 mm in both dimensions. Human skin was obtained from cosmetic surgeries and was kindly provided by Labtec by Adhex Pharma (Langenfeld, Germany).

### 2.2. Methods

#### 2.2.1. Preparation of microneedle array patches made from pure polymers

MAPs were prepared from the extended-release polymers Eudragit® RS, Eudragit® RL and ethyl cellulose to identify the polymers properties for the production of MAPs. Drug-free solutions were prepared. The compositions of these formulations are summarized in Table 1.

The polymers were dispersed in ethyl acetate and were stirred on a magnetic stirrer until clear solutions were obtained. Macrogol 400 was added to the ethyl cellulose-containing solution as a pore-forming agent. Ibuprofen was used as the model API. 1000.0 mg ibuprofen were added to 50.0 g of each drug-free formulation. F1, F2 and F3 were stirred until the API was completely dissolved. 50 µg of the drug-containing formulations were applied to a micromold and centrifugation was performed using the Multifuge 1L (Heraeus, Hanau, Germany). An exemplary micromold is shown in Fig. 1.

**Table 1**

Compositions of drug-free formulations containing extended-release polymers; ethyl acetate as the solvent.

Formulation	Polymer	Polymer concentration w/w [%]	Macrogol 400 % [w/w]
F1	Eudragit® RS	20.0	–
F2	Eudragit® RL	20.0	–
F3	Ethyl cellulose	20.0	2.0

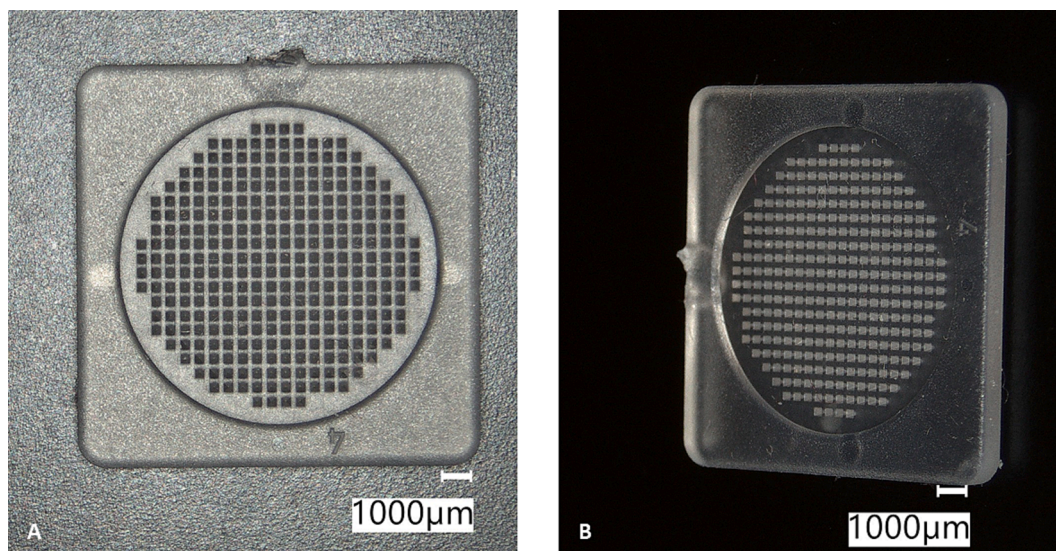


**Fig. 1.** Exemplary pictures of a micromold; A: top view, B: side view; each mold contained 300 cavities (650  $\mu\text{m}$  height, 300 x 300  $\mu\text{m}$  base, pyramidal shape).

The molds were centrifuged for 20 min at a speed of 4250 rpm (3776 g). The excess polymeric solution has been removed using a knife. After that, 150  $\mu\text{l}$  of the same drug-free formulation was applied to the mold using a pipette to form a coherent baseplate. The MAPs were dried using a desiccator filled with freshly activated silica gel at room temperature for 14 h. The dried patches were carefully removed from the mold. The manufacturing process of MAPs made from pure extended-release polymers is shown in Fig. 2.

### 2.2.2. Inkjet printing

Finding a suitable ink for the manufacturing process of dissolvable MAPs has been described before as well as finding suitable printing parameters (Lammerding and Breitzkreutz, 2023). The same ink has been used for printing purposes in this study. Briefly, 25.0 g povidone K17 were dispersed in 70.0 g demineralized water. The dispersion was stirred

on a magnetic stirrer until a clear solution was obtained. 1.0 g poly-sorbate 20 and 4.0 g glycerol 85 % were added and the solution was mixed. After that, 1050 mg lisinopril dihydrate were dissolved in 30.0 ml of the drug-free ink. Inkjet printing was performed using the desktop inkjet system PixDro LP50 (Meyer Burger, Eindhoven, The Netherlands). The inkjet printer was equipped with a piezo-driven drop-on-demand printhead with a nozzle diameter of 50  $\mu\text{m}$  (Spectra SL-128 AA, Fujifilm Dimatrix, Santa Clara, CA, USA). A pressure of  $-18.30$  mbar was applied to the ink reservoir and the temperature of the printhead was set to 30  $^{\circ}\text{C}$ . The jetting frequency was set to 500 Hz, the dwell time to 7.0  $\mu\text{s}$  and the pulse voltage to 100.0 V with a pulse shape of 90 %. Jetting was performed using a single nozzle.

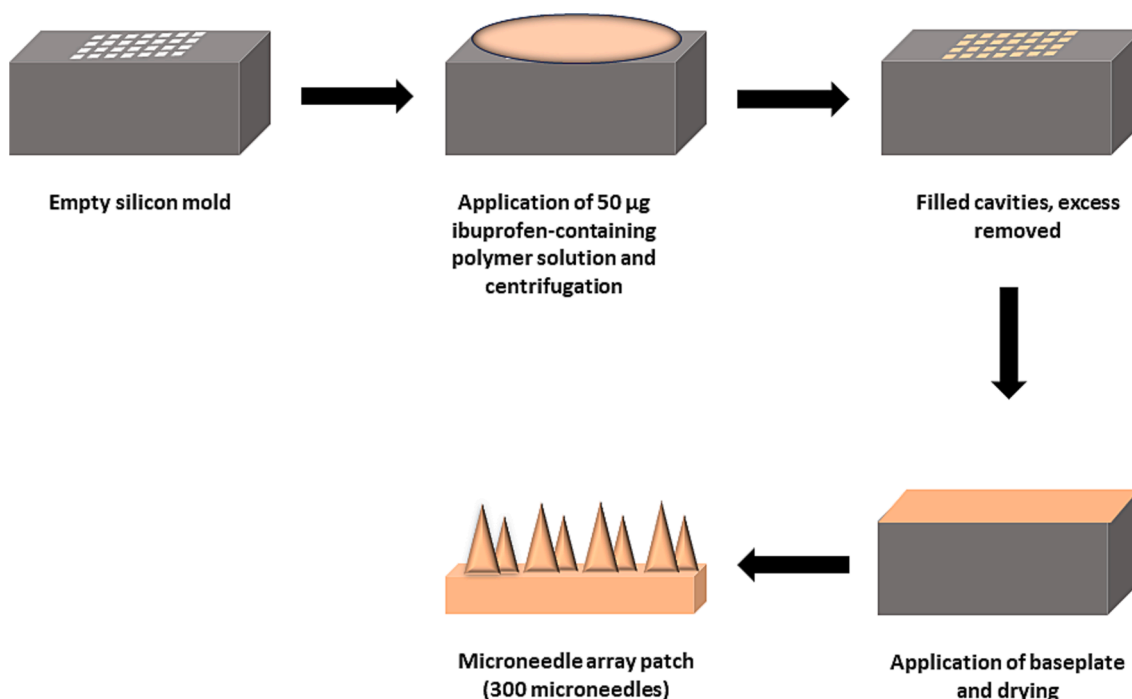


**Fig. 2.** Manufacturing of MAPs made from pure extended-release polymers using the centrifugation method; ibuprofen was included as a model API.

### 2.2.3. Preparation of microneedle array patches containing two spatially separated polymers

Inkjet printing and the centrifugation method described in section 2.2.1 were combined to manufacture MAPs containing two different polymers loaded with two different APIs. The upper half of the cavities (Fig. 3) was filled using inkjet printing. The droplet volume was measured using the camera system of the inkjet printer and the integrated software tool Advanced Drop Analysis (ADA, v2.4.2, Meyer Burger, Eindhoven, The Netherlands). The droplet volume was approx. 70  $\mu\text{l}$ .

360 drops of the ink described in section 2.2.2 were jetted per cavity in order to fill it completely. Drying was performed in a desiccator filled with freshly activated silica gel for 2 h after the upper half of the cavities of the micromold (150 cavities) were filled. The other half of the cavities were filled using the centrifugation method described in section 2.2.1. 50  $\mu\text{g}$  of the extended-release polymer-containing solution were added to the micromold. Centrifugation was performed at a speed of 4250 rpm (3776 g) for 20 min. The excess was carefully scraped off and 150  $\mu\text{l}$  of the same drug-free extended-release polymer solution were applied to form a coherent baseplate. Drying was performed in a desiccator filled with freshly activated silica gel at room temperature for 14 h. The dried MAPs were carefully released from the micromold. The manufacturing process is summarized in Fig. 4.

### 2.2.4. Visual inspection of MAPs

The digital light microscope VHX7000 (Keyence, Osaka, Japan) was used. Pictures of the MAPs were taken at different magnifications. Pictures displaying whole MAPs were taken using a zoom of 10 fold (whole MAPs) and 50 fold (single microneedles). MAPs were visually investigated before and after dissolution testing. The integrated measuring function of the microscope was used to determine the height of single microneedles.

### 2.2.5. Mechanical strength of microneedle array patches

The mechanical strength of MAPs has been determined using a method described by Larraneta et al. (Larraneta et al., 2014). A TA.XTplus texture analyser (Stable Micro Systems, Godalming, UK) was used. The microneedle array patches were attached with the needles down to the moveable probe of the texture analyser using double-sided adhesive tape and the texture analyser was set to compression mode. The moveable probe was moved downwards with a constant speed of 1.0 mm/s (pre-test speed) and the microneedles were pressed against the flat aluminum block of the texture analyser. The test started when the trigger force of 0.049 N was reached. The microneedles were pressed against the aluminum block with a constant force of 32 N with a speed of 0.5 mm/s (test speed). The force was held for 30 s. The moveable probe moved upwards with a speed of 1.0 mm/s after finishing the test (post-

test speed). The height of the microneedles was determined before and after the compression using the digital microscope VHX7000. Pictures of single needles were taken at a zoom of 50 fold. The percentage height reduction of the needles after compression testing was determined and used as an indicator of the mechanical stability. The test has been performed for MAPs made from pure extended-release polymer as well as for MAPs consisting of povidone and extended-release polymer. Six single needles were measured and arithmetic means ( $\bar{x}$ ) and standard deviations (sd) were calculated.

### 2.2.6. Penetration into Parafilm® M

The insertion behavior of MAPs into skin has been simulated using a method first described by Larraneta et al. (Larraneta et al., 2014). Eight layers of Parafilm® M (Bemis, Neenah, Wisconsin, USA) were used as an artificial skin membrane model. The MAPs were attached to the cylindrical moveable probe of the TA.XTplus texture analyser (Stable Micro Systems, Godalming, UK) like described in section 2.2.4. The texture analyser was set to compression mode. The probe was moved downwards until the needles reached the eight layers of Parafilm® M. A force of 32 N has been applied and held for 30 s when the trigger force of 0.049 N was reached. Pre- and post-test speed were set to 1.0 mm/s. The MAPs were carefully detached from the Parafilm® and the pierced single film layers were investigated using the digital microscope VHX7000. Pictures of the layers were taken and the pores created in each layer were counted. Testing the insertion was performed for MAPs prepared from pure extended-release polymers as well as for MAPs consisting of povidone and extended-release polymer. The test was performed in triplicate and arithmetic means ( $\bar{x}$ ) and standard deviations (sd) were calculated.

### 2.2.7. Dissolution testing

The lisinopril dihydrate and ibuprofen release from MAPs (MAPs made of an extended-release polymer and MAPs made of povidone and the extended-release polymer) were investigated using 3D-printed sample holders. The MAPs were attached to the sample holders using cyanoacrylate glue. The sample holders were placed in 15 ml vessels. Phosphate buffered saline (PBS) has been used as the dissolution medium. Therefore, 8.0 g sodium chloride, 0.2 g potassium chloride, 1.42 g disodium hydrogen phosphate and 0.27 g potassium dihydrogen phosphate were dissolved in 1.0 L demineralized water. The pH has been adjusted to 7.4 using phosphoric acid 85 %. 10.0 ml phosphate buffered saline pH 7.4 were filled into each vessel. The vessels were placed into a drying cabinet and the temperature was set to 37 °C. The complete MAPs were placed in the dissolution medium. The samples were stirred at a speed of 200 rpm during the dissolution studies. 1.0 ml of medium were taken as a sample at predefined time points (0, 5, 10, 15, 20, 30, 40, 50, 60, 90, 120, 150, 180, 240, 300, 360 and 1440 min for MAPs made of

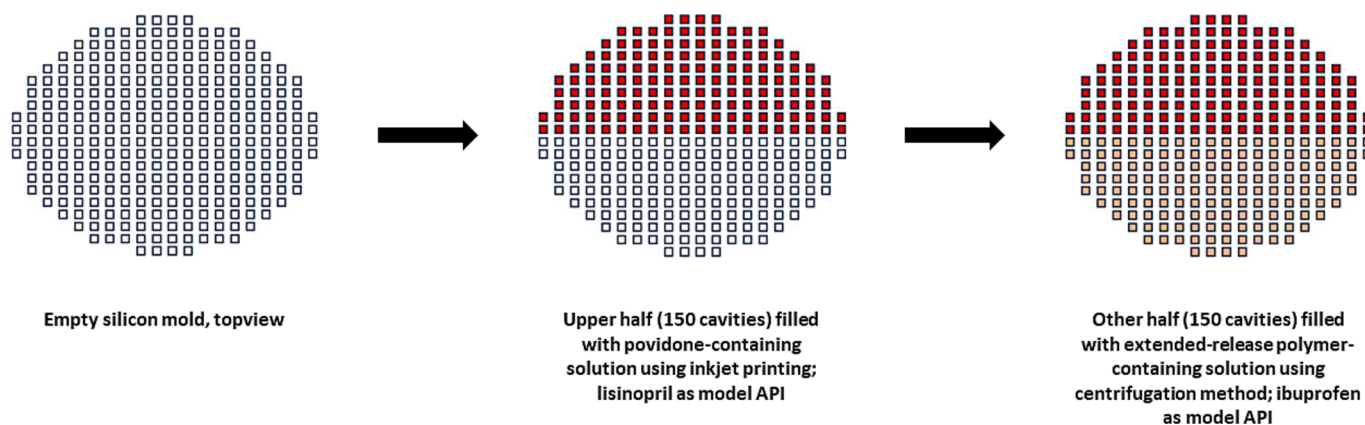


Fig. 3. Top view of the micromold; 300 cavities in total; upper half filled with povidone-containing ink and lisinopril using inkjet printing, lower half filled with extended-release polymer containing solution and ibuprofen using centrifugation method.

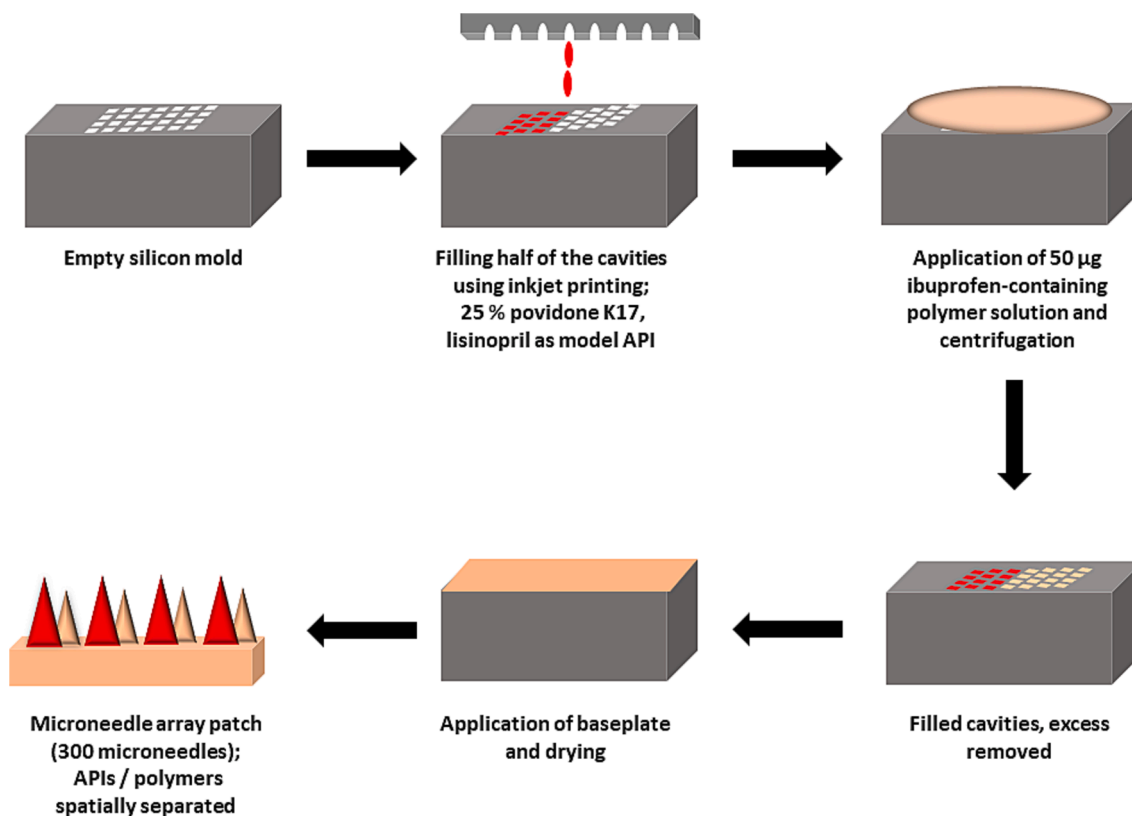


Fig. 4. Manufacturing of MAPs made of two different polymers (spatially separated); rapidly dissolving microneedles made of povidone containing lisinopril (red) and sustained release microneedles Eudragit® RS / RL.

pure extended-release polymers and 0, 1, 2, 3, 5, 7, 9, 11, 15, 20, 30, 60, 90, 120, 180, 240, 300, 360 and 1440 min for MAPs made of povidone and the extended-release polymers). The taken medium was replaced by 1.0 ml fresh phosphate buffered saline pH 7.4. The vessels were covered with Parafilm® M to avoid evaporation of the dissolution medium. All dissolution studies were performed in threefold. Arithmetic means ( $\bar{x}$ ) and standard deviations (sd) were calculated. The sample solutions were subjected to the HPLC assay described in section 2.2.10.

#### 2.2.8. Insertion into human skin

Skin samples were obtained from cosmetic surgeries and were kindly provided by Labtec by Adhexpharma (Langenfeld, Germany). The skin was cut into pieces of equal thickness using a dermatome (Integra Padgett Dermatome, Model S-Slimline, Integra LifeSciences, Ratingen, Germany). Every skin sample was cut into pieces with a thickness of 800–900  $\mu\text{m}$  to ensure that the microneedles did not pierce the whole skin. The SC was intact after dermatomization has been performed. The human skin was frozen and stored in a freezer at a temperature of  $-80\text{ }^{\circ}\text{C}$ . The skin was defrosted at room temperature directly before it was used. The skin was cut into circular pieces (diameter of 22 mm) using a hole punch.

MAPs made of povidone using inkjet printing and Eudragit® RS and RL were pierced into human skin using the force of a thumb. MAPs were pressed in the skin for 30 s. After that, the skin samples were rinsed with an aqueous methylene blue solution (1 % m/V). The skin was washed after 5 min using ethanol. The treated skin samples were investigated using the digital light microscope VHX 7000. This method is usually used to determine the ability of MAPs to pierce the skin (Li et al., 2009).

#### 2.2.9. In vitro skin permeation

The permeation of ibuprofen and lisinopril dihydrate was investigated using Franz-diffusion cells. Human skin samples were prepared like described in section 2.2.8. MAPs made of povidone using inkjet

printing and Eudragit® RS and RL using the centrifugation method were inserted into human skin (circular pieces, diameter of 22 mm) using the force of a thumb. The force was applied for 30 s. After that, the skin samples were attached to the Franz-diffusion cells using cyano acrylate glue. A stainless steel weight (25.0 g) was placed on the MAPs to keep the MAPs in place. The whole Franz-diffusion cell was covered with Parafilm® M to avoid evaporation of receiver medium. 11.5 ml of PBS (Adjusted to a pH of 7.4) was used as the medium in the receiver compartment. 1.0 ml were sampled at predefined time points (10, 20, 30, 60, 120, 180, 240, 360, 480 and 1440 min) and the medium was directly replaced with fresh and prewarmed PBS (adjusted to a pH of 7.4). Ex-vivo skin permeation was performed using a heating chamber at a temperature of  $37\text{ }^{\circ}\text{C}$ . The samples were constantly stirred using a stirring speed of 200 rpm. All permeations were performed six times. The samples were subjected to the HPLC assay described in section 2.2.10. The amount of ibuprofen and lisinopril permeated through human skin was determined and arithmetic means ( $\bar{x}$ ) and standard deviations (sd) were calculated.

#### 2.2.10. HPLC assay

The quantification of ibuprofen was performed using HPLC. An Agilent (1260 infinity, Agilent Technologies, Santa Clara, CA, USA) HPLC with diode array UV absorption detector was used. An isocratic method with reversed stationary phase (Knauer Eurosphere II 100–5 C18A, Berlin, Germany) was used. Mobile phase was sodium dihydrogen phosphate buffer (0.8 g/L adjusted to pH 3.5 with phosphoric acid 85 %) and acetonitrile (40:60). The flowrate was set to 1.0 ml/min and the detection was performed at a wavelength of 210 nm. The injection volume was set to 20  $\mu\text{l}$  and the column temperature to  $40\text{ }^{\circ}\text{C}$ . The retention time of ibuprofen was 3.6 min. This method was applied to samples of the dissolution study of MAPs made of pure extended-release polymers containing ibuprofen.

The quantification and separation of lisinopril dihydrate and

ibuprofen was performed using the same HPLC with the same equipment. A gradient elution method with reversed stationary phase (Knauer Eurosphere II 100–5 C18A, Berlin, Germany) was used. Sodium dihydrogen phosphate buffer (0.8 g/L adjusted to pH 3.5 with phosphoric acid 85 %) was used as mobile phase A and acetonitrile was used as mobile phase B, respectively. The method is summarized in Table 2.

Detection was performed using a wavelength of 210 nm. Injection volume was set to 20  $\mu$ l and the column temperature to 40 °C. The retention time of lisinopril dihydrate was determined to be 3.3 min and the retention time of ibuprofen 6.1 min, respectively.

### 3. Results and discussion

#### 3.1. Manufacturing of MAPs made from extended-release polymers

##### 3.1.1. Mechanical stability of MAPs made from extended-release polymers

MAPs manufactured from extended-release polymers (Eudragit® RS, Eudragit® RL and ethyl cellulose) were successfully produced using the centrifugation method. MAPs made from Eudragit® RS were sharp and intact after drying and had a height of  $651.97 \pm 6.51 \mu\text{m}$  (Fig. 6 C). The target height of the needles was 650  $\mu\text{m}$  and no significant shrinking was observed. MAPs made from Eudragit® RL had a height of  $648.64 \pm 3.34 \mu\text{m}$  showing no shrinking at all (Fig. 6 A). However, MAPs made from ethyl cellulose had a height of only  $558.00 \pm 37.34 \mu\text{m}$  (Fig. 6 E). These needles had no sharp tip and showed shrinking during drying. The results of testing the mechanical strength of MAPs made from pure extended-release polymers are shown in Fig. 5.

The height reduction after compression has been used to describe the mechanical stability of the microneedles. A force of 32 N was applied and held for 30 s. These are the average conditions during the application of MAPs (McAllister et al., 2003). Microneedles must not break during compression and breaking would result in excluding these MAPs from the test. The height reduction of microneedles made from Eudragit® RL was  $4.34 \pm 4.14 \%$ . The height reductions of MAPs made from Eudragit® RS and ethyl cellulose were  $13.91 \pm 2.07 \%$  and  $15.33 \pm 3.31 \%$ , respectively. It has been described that a height reduction below 10 % indicates a good stability of microneedles for sufficient transdermal drug delivery (Permana et al., 2021). Height reductions of more than 15 % are likely to result in very soft microneedles bending during application. The compression of microneedles against a surface made of aluminium is not completely comparable with the average conditions during the application of MAPs. It has been reported that height reductions larger than 15 – 20 % could result in a successful transdermal drug delivery (McCrudden et al., 2014). Furthermore, the relative height reduction of the microneedles indicating a sufficient mechanical stability is depending on the number of microneedles per MAP. The force applied per needle during the application is larger when MAPs with less microneedles are used. A relative height reduction of less than 10 % was determined to be sufficiently mechanically stable within the scope of this study. MAPs made from Eudragit® RL showed the smallest height reduction resulting in the most stable microneedles. These microneedles remained sharp and intact after compression and did not show any significant bending (Fig. 6 B). Therefore, microneedles made of Eudragit® RL were selected as an interesting approach for long-acting

**Table 2**

Gradient HPLC method for determination and separation of lisinopril and ibuprofen; mobile phase A was sodium dihydrogen phosphate buffer pH 3.5 and mobile phase B was acetonitrile.

Time [min]	A [%]	B [%]	Flow rate [ml/min]
0.00	85.0	15.0	1.0
1.50			
2.50	30.0	70.0	
8.00			
9.00	85.0	15.0	
12.00			

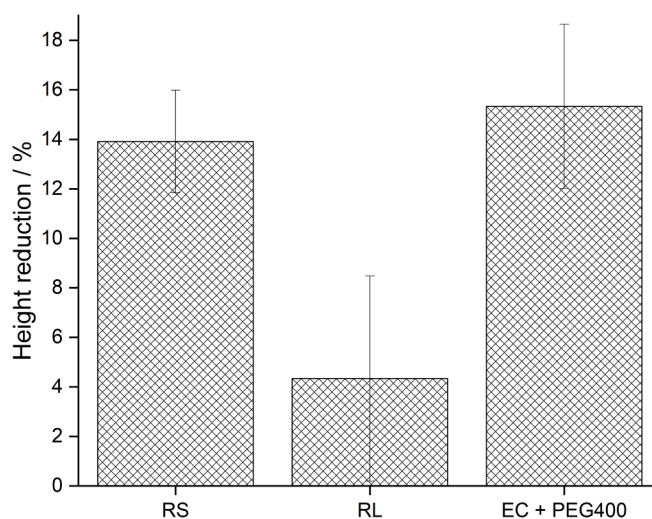


**Fig. 5.** Mechanical stability of MAPs made from pure extended-release polymers; RS = Eudragit® RS, RL = Eudragit® RL and EC + PEG 400 = Ethyl cellulose with PEG 400 as a pore forming agent;  $\bar{x} \pm \text{sd}$ , n = 6.

transdermal drug delivery using insoluble MAPs.

MAPs made from Eudragit® RS showed a larger height reduction compared to MAPs made from Eudragit® RL ( $13.91 \pm 2.07 \%$  vs.  $4.34 \pm 4.14 \%$ ). However, the microneedles still remained sharp and intact after compression (Fig. 6 D). Therefore, Eudragit® RS had been chosen as a polymer for the production of MAPs containing two APIs in two different polymers spatially separated.

The height reduction of microneedles made from ethyl cellulose showed the largest height reduction. The height reduction was  $15.33 \pm 3.31 \%$  (Fig. 5). The needle were too soft and bent during compression (Fig. 6 F).

The microneedles showed shrinking during drying. The height of single needles was  $558.00 \pm 37.34 \mu\text{m}$  before drying. Overall, MAPs manufactured using ethyl cellulose as the extended-release polymer in combination with macrogol 400 as a pore forming excipient were very soft. It could be expected that these microneedles are too soft to pierce the skin. Therefore, no MAPs combining two different polymers in one patch were produced using ethyl cellulose as the extended-release polymer.

##### 3.1.2. Penetration into Parafilm® M of MAPs made from extended-release polymers

The results of testing the insertion of MAPs made from pure extended-release polymers into eight layers of Parafilm® M are shown in Fig. 7. Microneedle array patches made from Eudragit® RS and RL pierced at least two layers of Parafilm® M. This is equal to an insertion depth of 254  $\mu\text{m}$ .  $89.73 \pm 5.93 \%$  of the microneedles consisting of Eudragit® RS reached that insertion depth and  $94.71 \pm 1.77 \%$  of the microneedles made of Eudragit® RL, respectively. It has been described that an insertion depth of at least two layers is necessary for a sufficient transdermal drug delivery using MAPs (Volpe-Zanutto et al., 2021). Furthermore, the shape, height and geometry of the microneedles play an crucial role for a successful transdermal drug delivery (Davidson et al., 2008). Both types of Eudragit® met this requirement.  $28.64 \pm 0.87 \%$  of the microneedles made of Eudragit® RS pierced the third layer of Parafilm® M. This is equal to an insertion depth of 381  $\mu\text{m}$ . The number of microneedles consisting of Eudragit® RL reaching an insertion depth of 381  $\mu\text{m}$  is comparable.  $17.52 \pm 2.96 \%$  of these needles pierced the third layer. MAPs made from ethyl cellulose containing PEG 400 as a pore forming excipient showed completely different results. Only  $22.08 \pm 10.71 \%$  of the microneedles pierced the second layer of Parafilm® M (equal to 254  $\mu\text{m}$ ) and no needles pierced the third layer (equal to 381  $\mu\text{m}$ ). This correlates to the results of the mechanical

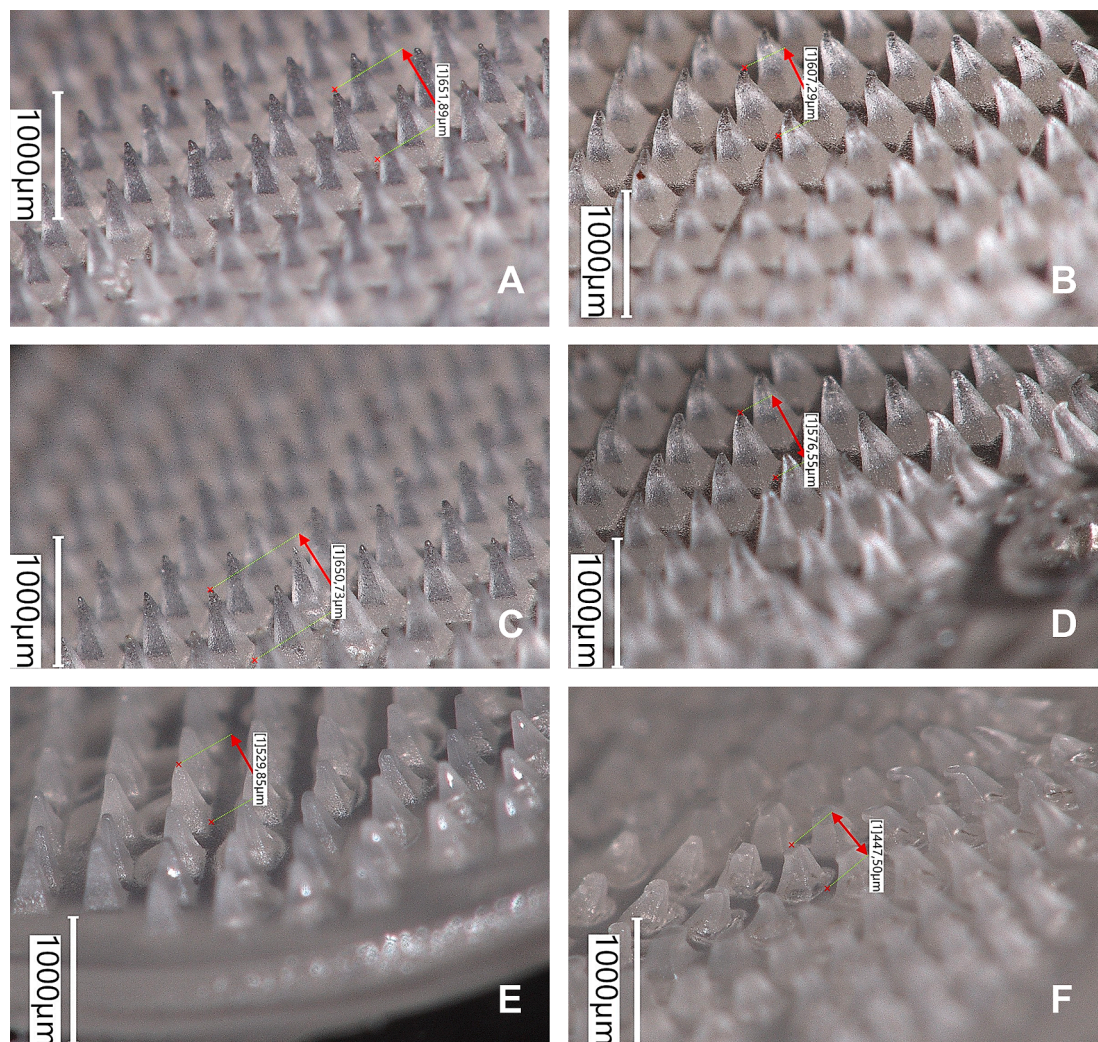


**Fig. 6.** Exemplary microneedles made from extended-release polymers before and after compression with 32 N for 30 s; A: Eudragit® RL before compression; B: Eudragit® RL after compression; C: Eudragit® RS before compression; D: Eudragit® RS after compression; E: Ethyl cellulose + PEG 400 before compression; F: Ethyl cellulose + PEG 400 after compression.

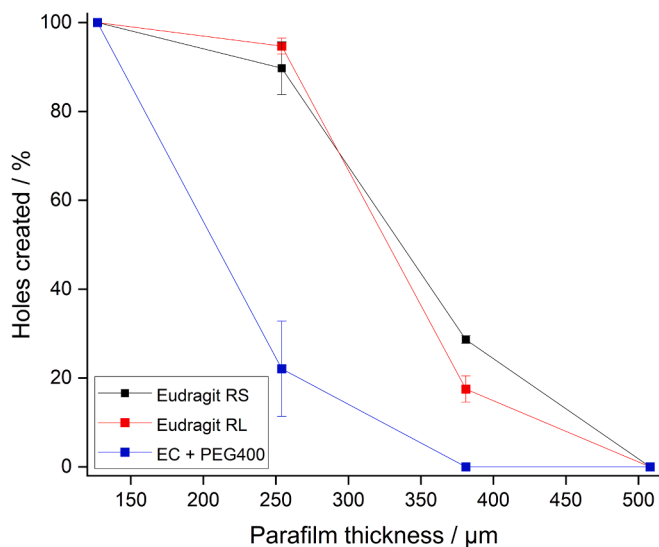


**Fig. 7.** Penetration of MAPs made from extended-release polymers into eight layers of Parafilm® M as an artificial skin membrane model;  $\bar{x} \pm \text{sd}$ ,  $n = 3$ .

stability testing (see section 3.1). MAPs made from ethyl cellulose were too soft and mechanically unstable. The needles bent during compression and could not pierce more than one layer of Parafilm® M. The pore former PEG 400 had additional plasticizing properties. Overall, MAPs made from ethyl cellulose were too soft to reach sufficient transdermal drug delivery. Therefore, no MAPs containing povidone as the water soluble polymer and ethyl cellulose as the extended-release polymer were further produced and characterized.

### 3.1.3. Dissolution of MAPs made from extended-release polymers

The dissolution profiles of ibuprofen from MAPs made of Eudragit® RS, Eudragit® RL and ethyl cellulose are shown in Fig. 8.

Ibuprofen showed the lowest dissolution rate from MAPs prepared from Eudragit® RS as the extended-release polymer (Fig. 8). 216.89  $\pm$  9.52  $\mu\text{g}$  (43.38  $\pm$  1.90 %) ibuprofen have been dissolved after 24 h. It could be assumed that the release of ibuprofen was still in process, as no plateau has been reached. The dissolution was very slow in the beginning as only 32.41  $\pm$  6.27  $\mu\text{g}$  (6.48  $\pm$  1.25 %) ibuprofen were dissolved after 60 min and 50.90  $\pm$  9.00  $\mu\text{g}$  (10.18  $\pm$  1.80 %) after 120 min, respectively. Eudragit® RS is less permeable compared to Eudragit® RL. 472.49  $\pm$  34.02  $\mu\text{g}$  (94.50  $\pm$  6.80 %) ibuprofen were dissolved after 24 h when Eudragit® RL was used as the extended-release polymer for microneedle production (Fig. 8). However, the dissolution of ibuprofen has been mostly finished after 360 min. 405.77  $\pm$  14.15  $\mu\text{g}$  (81.15  $\pm$

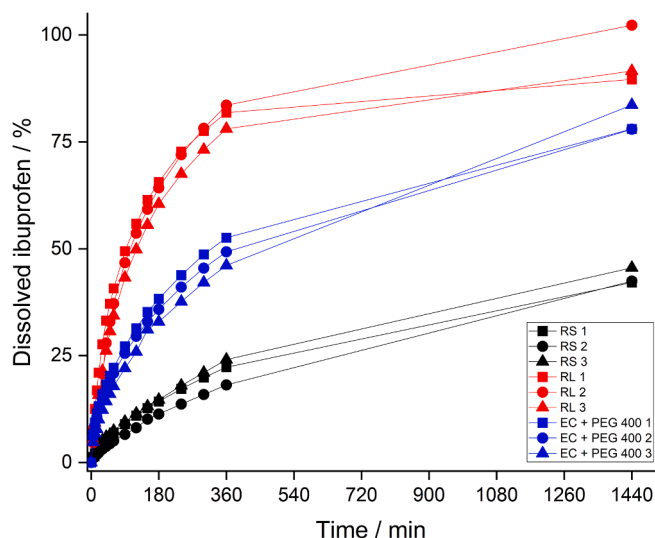


**Fig. 8.** Dissolution profiles of ibuprofen from MAPs made of pure extended-release polymers (A: Eudragit® RS, B: Eudragit® RL, C: Ethyl cellulose with PEG 400 as pore forming excipient); single curves,  $n = 3$ ; media: PBS (adjusted to a pH of 7.4 and a temperature of 37 °C).

2.83 %) ibuprofen were dissolved after 360 min. The dissolution rate was much faster compared to MAPs made from Eudragit® RS, especially in the beginning.  $187.05 \pm 15.94 \mu\text{g}$  ( $37.41 \pm 3.19 \%$ ) ibuprofen were dissolved after 60 min and  $265.59 \pm 15.29 \mu\text{g}$  ( $53.12 \pm 3.06 \%$ ) after 120 min, respectively. MAPs made from ethyl cellulose containing PEG 400 as a pore forming excipient showed a dissolution profile somewhere between both Eudragit® types (Fig. 8).  $399.36 \pm 16.26 \mu\text{g}$  ( $79.87 \pm 3.25 \%$ ) ibuprofen were dissolved after 24 h and  $101.48 \pm 11.11 \mu\text{g}$  ( $20.30 \pm 2.22 \%$ ) after 60 min and  $144.67 \pm 14.06 \mu\text{g}$  ( $28.93 \pm 2.81 \%$ ) after 120 min, respectively. That indicates that the dissolution of ibuprofen using ethyl cellulose as the extended-release polymer is slower compared to MAPs made from Eudragit® RL but faster compared to MAPs made from Eudragit® RS. It could be demonstrated that an adjustment of the dissolution behavior was possible using the three different polymers. Even though ethyl cellulose showed good characteristics in terms of drug release, the mechanical properties of these MAPs were insufficient. Therefore, no microneedle array patches were made containing povidone in combination with ethyl cellulose. Eudragit® RS and RL were selected as suitable polymers for the production of MAPs containing two different APIs in one patch spatially separated. Both polymers showed sufficient mechanical properties. The dissolution profiles were completely different offering the possibility for a wide range of application times.

### 3.2. Spatial separation of drug substances / polymers in one MAP

#### 3.2.1. Microscopic inspection of MAPs made by combining inkjet printing and micromolding

MAPs made by inkjet printing in combination with the centrifugation method were successfully produced. MAPs containing ibuprofen embedded in Eudragit® RS or Eudragit® RL as the extended-release polymers and spatially separated povidone containing lisinopril are shown in Fig. 9.

The microneedles were sharp and intact after manufacturing using both inkjet printing and the centrifugation method. To obtain information regarding the spatial separation of the polymers, the MAPs were placed in water for 10 min. The results for both extended-release polymers are shown in Fig. 10.

One half of the microneedles was completely dissolved after 10 min in water and the other half was unaltered. Microneedles made by inkjet printing dissolved quickly because the water-soluble polymer povidone has been used. On the other hand, the microneedles produced using the centrifugation method were made of the water-insoluble polymers Eudragit® RS and Eudragit® RL. Therefore, these 150 microneedles did not dissolve in water. A clear separation of dissolved and undissolved microneedles is visible (Fig. 10 A and B). It can be concluded that a spatial separation of different polymers forming microneedles in one MAP is possible using a combination of inkjet printing and the centrifugation method. It is important that the cavities filled using inkjet printing are not redissolved by the solvent of the extended-release polymer solution. Therefore, ethyl acetate was used as a solvent for Eudragit® RS and RL, whereas povidone is insoluble in this solvent. Overall, the controlled separation of different APIs in different microneedles is an interesting option to incorporate incompatible APIs in one MAP. Another approach is the combination of both polymers in one MAP using inkjet printing for both formulations. However, the viscosities of all formulations containing extended-release polymers in a sufficient concentration were too high to perform inkjet printing using the describe desktop inkjet printer.

#### 3.2.2. Mechanical stability of MAPs made by combining inkjet printing and micromolding

The results of testing the mechanical stability of MAPs made from povidone and extended-release polymers are shown in Fig. 11. MAPs containing Eudragit® RS and Eudragit® RL had a comparable height reduction of  $8.09 \pm 3.34 \%$  and  $8.30 \pm 1.10 \%$ , respectively. Both values are below 10 % which is below the described requirement to ensure a sufficient transdermal drug delivery. All microneedles remained sharp and intact after the compression (Fig. 12).

It can be concluded that both extended-release polymers showed good mechanical stability. The microneedles did not break during compression and remained intact. The height reduction was below 10 %. That indicated that the needles did not bend during compression. Overall, both polymers are promising candidates for transdermal drug delivery using MAPs.

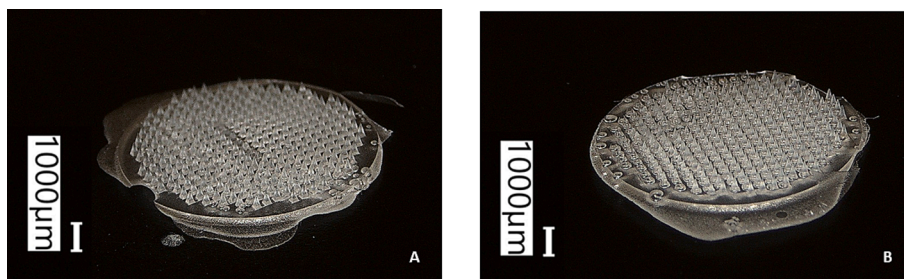


**Fig. 9.** MAPs made by combining inkjet printing and micromolding (centrifugation method) directly after drying (A: MAPs containing Eudragit® RS and povidone; B: MAPs containing Eudragit® RL and povidone); pictures taken at a zoom of 10 fold, scale bar represents 1000  $\mu\text{m}$ .

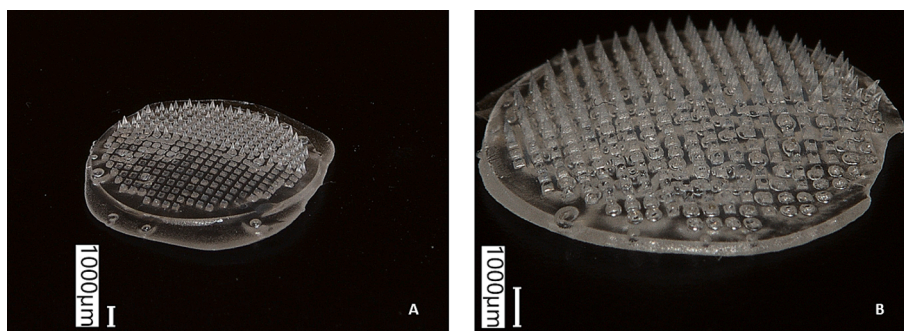


Fig. 10. MAPs made by combining inkjet printing and micromolding (centrifugation method) after 10 min in water (A: MAPs containing Eudragit® RS and povidone, zoom: 10 fold; B: MAPs containing Eudragit® RL and povidone, zoom: 20 fold); scale bar: 1000 µm.

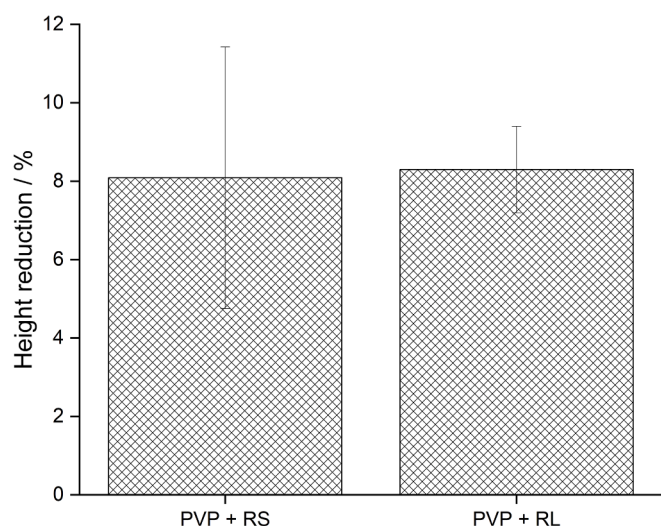


Fig. 11. Mechanical stability of MAPs made from povidone and extended-release polymers; PVP + RS = povidone and Eudragit® RS, PVP + RL = povidone and Eudragit® RL;  $\bar{x} \pm s$ , n = 6.

### 3.2.3. Penetration into Parafilm® M of MAPs made by combining inkjet printing and micromolding

The results of the insertion into eight layers of Parafilm® M as an artificial skin membrane model are shown in Fig. 13.

All microneedles pierced the first layer of Parafilm®. MAPs made from povidone and Eudragit® RS showed comparable results to MAPs made from povidone and Eudragit® RL.  $97.14 \pm 3.76$  % (Eudragit® RS) and  $97.50 \pm 2.13$  % (Eudragit® RL) of the microneedles pierced the second layer. That is equivalent to an insertion depth of 254 µm and is

the minimum limit described to ensure a sufficient transdermal drug delivery (Volpe-Zanutto et al., 2021).  $24.53 \pm 4.14$  % of the microneedles (povidone and Eudragit® RS) pierced the third layer of Parafilm® M which is equivalent to an insertion depth of 381 µm. The number of microneedles made from povidone and Eudragit® RL that could pierce the third layer was slightly higher ( $34.57 \pm 0.53$  %) but still comparable. It has been described before that microneedles made of different types of Eudragit® could pierce porcine skin (Aung et al., 2021; Aung et al., 2023). The results obtained in this study are comparable to the results described before. Nevertheless, the microneedles described in literature are made from pure polymers or mixtures of povidone and Eudragit®. It is interesting that the results of the polymers spatially separated are comparable.

### 3.2.4. Dissolution of MAPs made by combining inkjet printing and micromolding

The results of the dissolution testing of MAPs made from povidone as the water-soluble polymer and Eudragit® RS and RL as the extended release polymer are shown in Fig. 14.

Lisinopril was embedded in the microneedles made from povidone. Povidone is a polymer rapidly dissolving in water. Therefore, the lisinopril was dissolved almost completely after 9 min.  $128.09 \pm 15.76$  µg ( $99.89 \pm 12.29$  %) of lisinopril were dissolved from MAPs combined with microneedles containing Eudragit® RS and  $135.21 \pm 4.70$  µg ( $99.85 \pm 2.49$  %) from MAPs combined with microneedles containing Eudragit® RL after 20 min.  $132.14 \pm 47.47$  µg Lisinopril (in combination with Eudragit® RS) and  $135.02 \pm 3.34$  µg (in combination with Eudragit® RL) were dissolved after 24 h, respectively. Ibuprofen was embedded in the microneedles made from the extended-release polymers. The dissolution from these microneedles showed comparable results to dissolution from the MAPs made of extended-release polymers (Fig. 8 in section 3.1.3). Ibuprofen showed a slower dissolution from microneedles made from Eudragit® RS compared to Eudragit® RL.

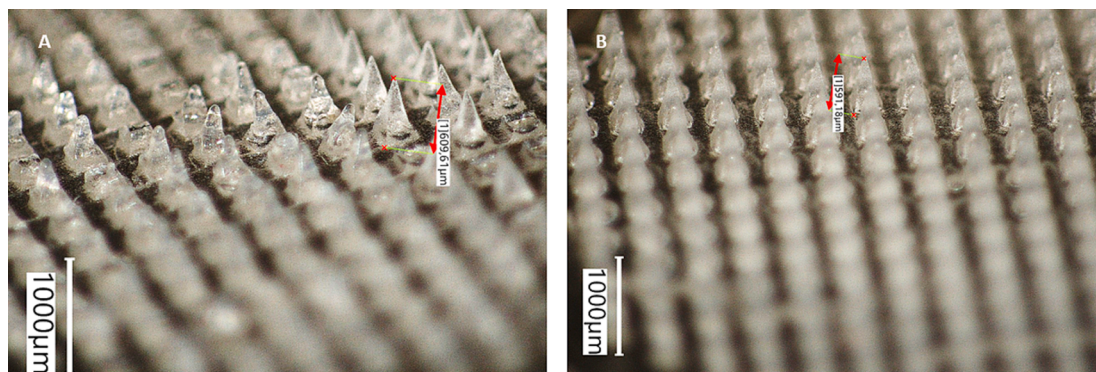


Fig. 12. MAPs made of povidone as the water-soluble polymer and Eudragit® RS (A) and RL (B) as the extended-release polymers after compression with 32 N for 30 s.

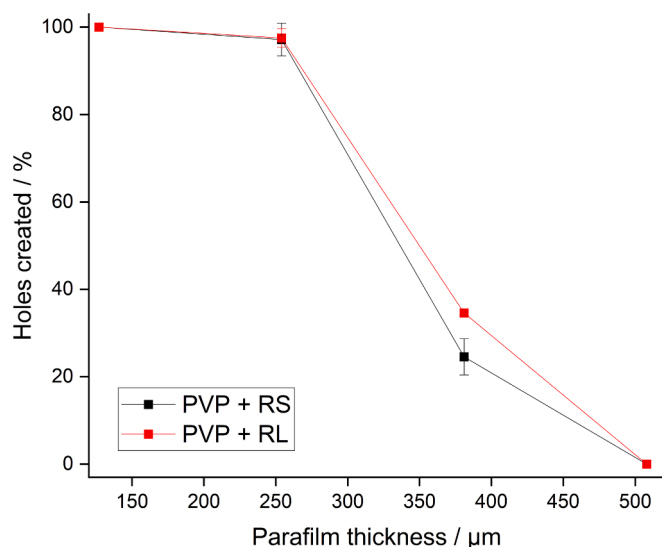


Fig. 13. Penetration of MAPs made of povidone as the water-soluble polymer and Eudragit® RS and RL as the extended-release polymers into Parafilm® M as an artificial skin membrane model;  $\bar{x} \pm \text{sd}$ ,  $n = 3$ .

$39.78 \pm 7.67 \mu\text{g}$  ibuprofen (Eudragit® RS) were dissolved after 20 min. After the same time  $115.26 \pm 5.33 \mu\text{g}$  were already dissolved from the microneedles made of Eudragit® RL. Approx. 80 % of the ibuprofen ( $445.16 \pm 9.98 \mu\text{g}$ ) were dissolved after 6 h from the MAPs containing Eudragit® RL as the extended-release polymer. On the other hand, only  $122.91 \pm 21.30 \mu\text{g}$  ibuprofen were dissolved from the MAPs containing Eudragit® RS after the same period of time (Fig. 14 A). After 24 h,  $211.80 \pm 22.98 \mu\text{g}$  ibuprofen (Eudragit® RS) and  $560.09 \pm 18.29 \mu\text{g}$  (Eudragit® RL) were dissolved, respectively. It can be concluded that combining inkjet printing and the centrifugation method (micro-molding) is a possibility to combine different APIs embedded in polymers with different dissolution profiles. This may lead to an increase in the patients adherence since the number of drug products to take may be reduced.

### 3.2.5. Insertion into human skin

Successful piercing of an artificial skin model was demonstrated for

the manufactured MAPs containing microneedles made of povidone and Eudragit® RS or RL spatially separated from each other (section 3.2.3). However, this skin model was only compared with porcine skin and showed similar mechanical properties (Larraneta et al., 2014). Human skin has different mechanical properties compared to porcine skin.

The penetration behavior into human skin was investigated. For this purpose, human skin was stained with the water-soluble dye methylene blue after application of the MAPs. The SC represents the lipophilic barrier of the skin. After washing off the dye, the SC is decolorized again. However, if micropores are formed in the skin due to the application of the MAPs, these are more hydrophilic. The dye cannot be easily washed out of these pores and the pores are of a more intense blue color (McCrudden et al., 2014; Tekko et al., 2020).

The results of the insertion of MAPs into human skin are shown in Fig. 15.

Both MAPs successfully pierced the SC. After washing off the excessive methylene blue solution, the individual micropores caused by the microneedles were clearly recognizable. Povidone is a well-studied polymer for the production of dissolvable MAPs. Various APIs have already been applied transdermally using povidone microneedles (Carcamo-Martinez et al., 2021; Chen et al., 2020; Dali and Shende, 2023). These MAPs successfully pierced the skin. However, these studies were carried out with porcine or mouse skin. The microneedles produced in this study showed comparable results and successfully pierced human skin.

The production of microneedles from Eudragit® RS and RL is less common. Eudragit® RS was used in combination with povidone for successful delivering resveratrol transdermally (Aung et al., 2021). These microneedles pierced porcine skin. Eudragit® RL was characterized to successfully deliver granisetron transdermally (Yang et al., 2018).

The MAPs produced and characterized in this work exhibited similar properties to MAPs made from the same polymers described in the literature. The microneedles were mechanically robust enough to pierce human skin even after spatial separation. This implied a possible use of these MAPs for the transdermal delivery of two drug substances using one single MAP. However, it is possible that some microneedles penetrate the skin deeper compared to other microneedles during the application. The separation of both polymers could be problematic if the force during application is not the same for each needle. It has been shown that inkjet printing is a feasible tool to fill cavities of a micromold

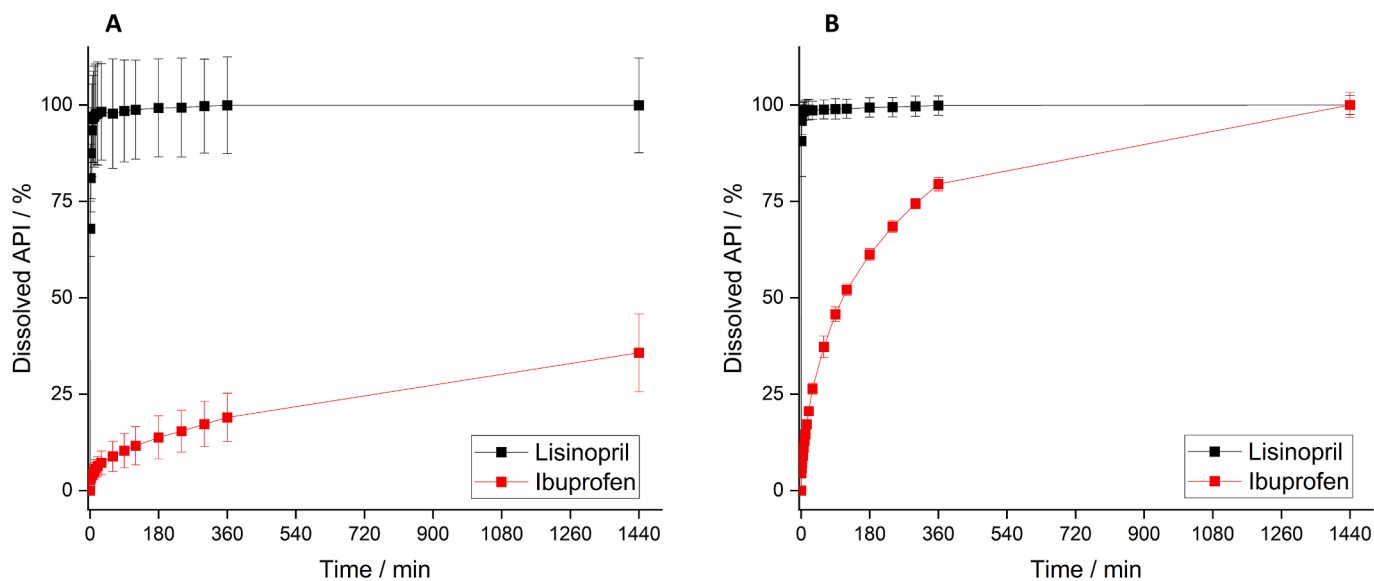


Fig. 14. Dissolution profiles of ibuprofen and lisinopril from MAPs made of povidone and Eudragit® RS (A) and RL (B); lisinopril was embedded in povidone and ibuprofen in Eudragit® RS and RL;  $\bar{x} \pm \text{sd}$ ,  $n = 3$ ; media: PBS (adjusted to a pH of 7.4 and an temperature of 37 °C).

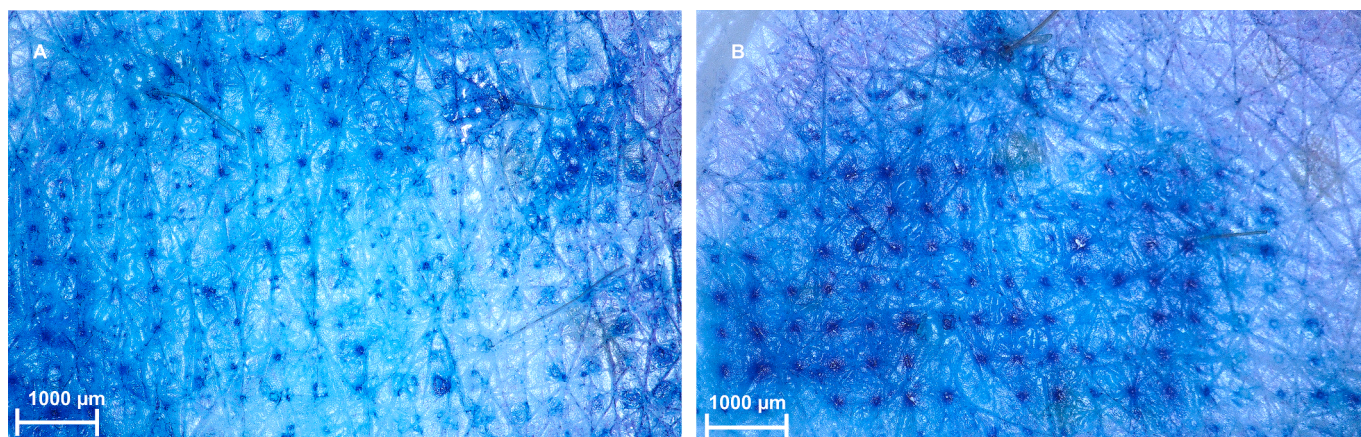


Fig. 15. Insertion of MAPs made of povidone and Eudragit® RS (A) and RL (B) into human skin; microscopic pictures taken at a zoom of 20 fold, scale bar represents 1000 µm.

individually (Lammerding and Breitzkreutz, 2023). It may be possible to fill every second cavity using inkjet printing and perform centrifugation afterwards. That could result in an even distribution of both APIs and increase the potential for a successful transdermal drug delivery during application.

### 3.2.6. In vitro skin permeation

Both MAPs were subjected to in vitro skin permeation studies (section 2.9). The results of determining the permeation of lisinopril dihydrate and ibuprofen across human skin are shown in Fig. 16.

It was feasible to administer lisinopril dihydrate and ibuprofen transdermally using the produced MAPs. Both MAPs showed comparable results to deliver lisinopril dihydrate using rapidly dissolving microneedles made from povidone.  $66.33 \pm 15.18 \mu\text{g}$  lisinopril dihydrate permeated across human skin using MAPs made from povidone and Eudragit® RS (Fig. 16 A) after 24 h and  $65.25 \pm 12.69 \mu\text{g}$  made from povidone and Eudragit® RL (Fig. 16 B), respectively. The permeation of ibuprofen was depending on the insoluble polymer used for the manufacturing of the MAPs. Using Eudragit® RS resulted in a slower permeation of ibuprofen ( $45.28 \pm 5.58 \mu\text{g}$ ) compared to microneedles made from Eudragit® RL ( $66.90 \pm 28.37$ ). These results are similar to the dissolution studies described before (section 3.2.4). An explanation for these results is the lower permeability of Eudragit® RS for APIs

compared to Eudragit® RL (Thakral et al., 2013).

The manufacturing of povidone microneedles containing lisinopril dihydrate has been described before (Quinn et al., 2015). The results obtained in this work are comparable to the results described in literature. Lisinopril was successfully delivered using dissolving microneedles for 24 h.

Overall, the manufacturing of MAPs containing two spatial separated drug substances embedded in two different polymers was feasible using a combination of inkjet printing and a centrifugation method. Both APIs permeated successfully across human skin.

## 4. Conclusion

It was possible to combine the inkjet printing and the centrifugation methods to manufacture MAPs containing two different APIs embedded in two different polymers. Povidone K17 was used for production of rapidly dissolving microneedles containing lisinopril dihydrate as a peptidomimetic API by inkjet printing. Ibuprofen has been used as a model API for small molecules and was incorporated into the polymethacrylates Eudragit® RS and RL. These polymers showed extended-release dissolution over a period of at least 24 h (Eudragit® RS) and approx. 6 h (Eudragit® RL), respectively. On the other hand, lisinopril-containing microneedles made from povidone dissolved and released

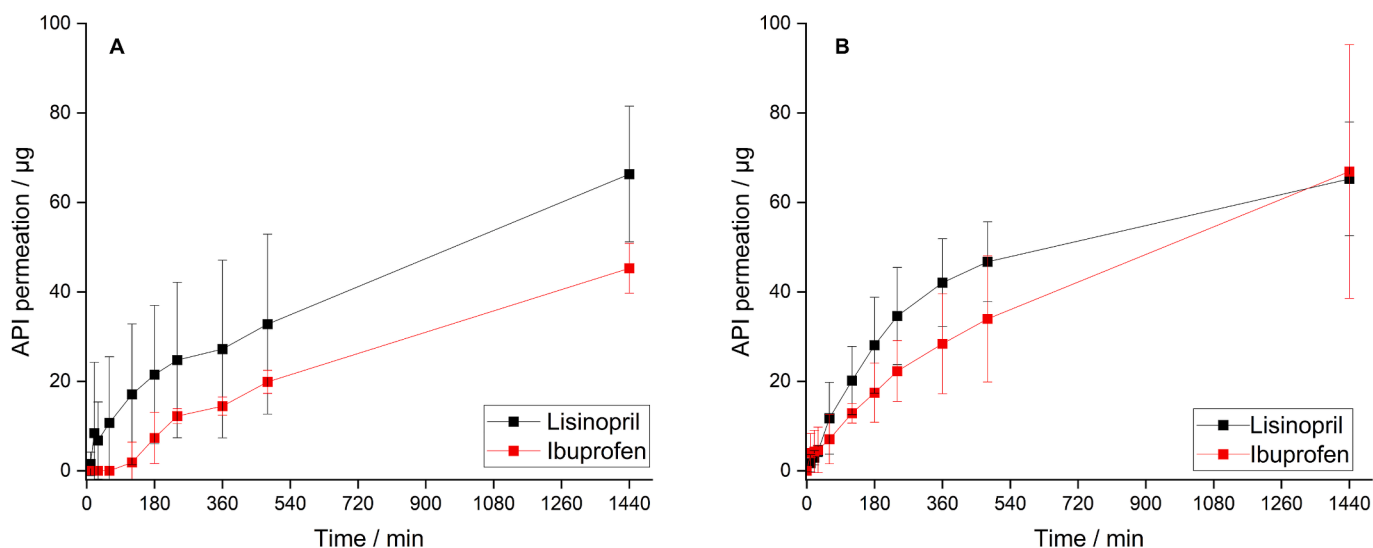


Fig. 16. In vitro permeation of ibuprofen and lisinopril from MAPs made of povidone and Eudragit® RS (A) and RL (B) across human skin; lisinopril was embedded in povidone and ibuprofen in Eudragit® RS and RL;  $\bar{x} \pm \text{sd}$ ,  $n = 6$ ; media: PBS (adjusted to a pH of 7.4 and a temperature of 37 °C).

the drug substance completely after approx. 10 min. A sharp and clear separation between the needles combined in one patch has been observed. Both MAPs enabled the permeation of the drug substances lisinopril dihydrate and ibuprofen across human skin. Microneedles made from povidone and microneedles made from the extended-release polymers were spatially separated. This could enable the combination of incompatible APIs in one patch. Another approach to spatially separate different polymers in one MAP is the use of inkjet printing without performing centrifugation afterwards. A successful printing process was limited to ink formulations of low viscosities in this study. Further investigations using a different inkjet printing system must be performed to get more information about a successful spatial separation using this approach. The combination of APIs in one dosage form may increase the patients adherence to the therapy since the number of applied drug products might be reduced. It is important to perform inkjet printing before filling the other cavities using the centrifugation method as it enables filling of single cavities and therefore highly precise dosing. Furthermore, the polymer filled in cavities using inkjet printing must not dissolve during the application of the second polymer. Further investigations should show if the combination of both methods is applicable to pharmaceutical relevant APIs in relevant dosages. Lisinopril and ibuprofen were used as model drug substances in this study. The content of both APIs is limited to a few micrograms. That is no pharmaceutically relevant dosage for both APIs. Lisinopril and ibuprofen were used as model drug substances for high potent drugs like vaccines, cytostatics or hormones. This are low-dosed APIs and a precise and constant dosing is crucial. A verification of the process for incompatible APIs is needed as well. Furthermore, it has been reported for oral film formulations that migration of drugs is possible between different polymer layers (Göbel and Breitzkreutz, 2022). Further investigations should show if the APIs migrate in the baseplate of the MAPs. However, a mixture of different amounts of both extended-release polymers could lead to the desired dissolution profiles and dose intervals.

#### CRedit authorship contribution statement

**Lukas C. Lammerding:** Writing – original draft, Investigation, Formal analysis, Conceptualization. **Awadhi Arora:** Investigation, Formal analysis. **Sebastian Braun:** Writing – review & editing, Supervision. **Jörg Breitzkreutz:** Writing – review & editing, Supervision.

#### Declaration of competing interest

The authors declare that they have no known competing financial interests or personal relationships that could have appeared to influence the work reported in this paper.

#### Acknowledgements

The authors would like to thank LTS Lohmann Therapie-Systeme for kindly providing the silicon molds for the production of microneedle array patches. Dr. Tobias Auel and Christofer Mentrup (Heinrich Heine University, Duesseldorf) are acknowledged for preparing sample holders for the dissolution studies by fused deposition modeling (3D printing). The authors would like to thank Dr. Tobias Tellkamp-Schehr (Labtec by Adhexpharma, Langenfeld, Germany) for providing and dematomizing the skin samples.

#### Data availability

Data will be made available on request.

#### References

- Alkilani, A.Z., McCrudden, M.T., Donnelly, R.F., 2015. Transdermal drug delivery: Innovative pharmaceutical developments based on disruption of the barrier properties of the stratum corneum. *Pharmaceutics* 7, 438–470.
- Allen, E.A., O'Mahony, C., Cronin, M., O'Mahony, T., Moore, A.C., Crean, A.M., 2016. Dissolvable microneedle fabrication using piezoelectric dispensing technology. *Int. J. Pharm.* 500, 1–10.
- Altuntas, E., Tekko, I.A., Vora, L.K., Kumar, N., Brodsky, R., Chevallier, O., McAlister, E., Kurnia Anjani, Q., McCarthy, H.O., Donnelly, R.F., 2022. Nestorone nanosuspension-loaded dissolving microneedles array patch: A promising novel approach for “on-demand” hormonal female-controlled peritocoital contraception. *Int. J. Pharm.* 614, 121422.
- Angkawitwong, U., Courtenay, A.J., Rodgers, A.M., Larraneta, E., McCarthy, H.O., Brocchini, S., Donnelly, R.F., Williams, G.R., 2020. A novel transdermal protein delivery strategy via electrohydrodynamic coating of PLGA microparticles onto microneedles. *ACS Appl. Mater. Interfaces* 12, 12478–12488.
- Aung, N.N., Ngawhirunpat, T., Rojanarata, T., Patrojanasophon, P., Opanasopit, P., Pamornpathomkul, B., 2019. HPMC/PVP dissolving microneedles: A promising delivery platform to promote trans-epidermal delivery of alpha-arbutin for skin lightening. *AAPS PharmSciTech* 21, 25.
- Aung, N.N., Ngawhirunpat, T., Rojanarata, T., Patrojanasophon, P., Opanasopit, P., Pamornpathomkul, B., 2021. Enhancement of transdermal delivery of resveratrol using Eudragit and polyvinyl pyrrolidone-based dissolving microneedle patches. *J. Drug Deliv. Sci. Technol.* 61, 102284.
- Aung, N.N., Pengnam, S., Ngawhirunpat, T., Rojanarata, T., Patrojanasophon, P., Opanasopit, P., Pamornpathomkul, B., 2023. Fabrication of polyvinyl pyrrolidone-K90/Eudragit RL100-based dissolving microneedle patches loaded with alpha-arbutin and resveratrol for skin depigmentation. *Biomater. Sci.* 11, 4583–4601.
- Bal, S.M., Kruthof, A.C., Zwier, R., Dietz, E., Bouwstra, J.A., Lademann, J., Meinke, M.C., 2010. Influence of microneedle shape on the transport of a fluorescent dye into human skin in vivo. *J. Control. Release* 147, 218–224.
- Carcamo-Martinez, A., Mallon, B., Anjani, Q.K., Dominguez-Robles, J., Utomo, E., Vora, L.K., Tekko, I.A., Larraneta, E., Donnelly, R.F., 2021. Enhancing intradermal delivery of tofacitinib citrate: Comparison between powder-loaded hollow microneedle arrays and dissolving microneedle arrays. *Int. J. Pharm.* 593, 120152.
- Chen, Z., Han, B., Liao, L., Hu, X., Hu, Q., Gao, Y., Qiu, Y., 2020. Enhanced transdermal delivery of polydatin via a combination of inclusion complexes and dissolving microneedles for treatment of acute gout arthritis. *J. Drug Deliv. Sci. Technol.* 55, 101487.
- Cheow, W.S., Kiew, T.Y., Hadinoto, K., 2015. Combining inkjet printing and amorphous nanonization to prepare personalized dosage forms of poorly-soluble drugs. *Eur. J. Pharm. Biopharm.* 96, 314–321.
- Chu, L.Y., Prausnitz, M.R., 2011. Separable arrowhead microneedles. *J. Control. Release* 149, 242–249.
- Dali, P., Shende, P., 2023. Use of 3D applicator for intranasal microneedle arrays for combinational therapy in migraine. *Int. J. Pharm.* 635, 122714.
- Davidson, A., Al-Qallaf, B., Das, D.B., 2008. Transdermal drug delivery by coated microneedles: Geometry effects on effective skin thickness and drug permeability. *Chem. Eng. Res. Des.* 86, 1196–1206.
- Frohoff-Hulsmann, M.A., Schmitz, A., Lippold, B.C., 1999. Aqueous ethyl cellulose dispersions containing plasticizers of different water solubility and hydroxypropyl methylcellulose as coating material for diffusion pellets. I. Drug release rates from coated pellets. *Int. J. Pharm.* 177, 69–82.
- Göbel, A., Breitzkreutz, J., 2022. Concept of orodispersible or mucoadhesive “Tandem Films” and their pharmaceutical realization. *Pharmaceutics* 14, 264.
- Jiang, J., Gill, H.S., Gbate, D., McCarey, B.E., Patel, S.R., Edelhauser, H.F., Prausnitz, M.R., 2007. Coated microneedles for drug delivery to the eye. *Invest. Ophthalmol. Vis. Sci.* 48, 4038–4043.
- Kang, N.W., Kim, S., Lee, J.Y., Kim, K.T., Choi, Y., Oh, Y., Kim, J., Kim, D.D., Park, J.H., 2021. Microneedles for drug delivery: Recent advances in materials and geometry for preclinical and clinical studies. *Expert Opin. Drug Deliv.* 18, 929–947.
- Kathuria, H., Lim, D., Cai, J., Chung, B.G., Kang, L., 2020. Microneedles with tunable dissolution rate. *ACS Biomater. Sci. Eng.* 6, 5061–5068.
- Kaushik, S., Hord, A.H., Denson, D.D., McAllister, D.V., Smitra, S., Allen, M.G., Prausnitz, M.R., 2001. Lack of pain associated with microfabricated microneedles. *Anesth. Analg.* 92, 502–504.
- Kim, M.J., Park, S.C., Rizal, B., Guanés, G., Baek, S.K., Park, J.H., Betz, A.R., Choi, S.O., 2018. Fabrication of circular obelisk-type multilayer microneedles using micro-milling and spray deposition. *Front. Biotechnol.* 6, 54.
- Lammerding, L.C., Braun, S., Breitzkreutz, J., 2023. Multilayer microneedle array patches by combining inkjet printing and micromolding - A technical evaluation. *Tanns. AMMM* 5, 798.
- Lammerding, L.C., Breitzkreutz, J., 2023. Technical evaluation of precisely manufacturing customized microneedle array patches via inkjet drug printing. *Int. J. Pharm.* 642, 123173.
- Larraneta, E., Moore, J., Vicente-Perez, E.M., Gonzalez-Vazquez, P., Lutton, R., Woolfson, A.D., Donnelly, R.F., 2014. A proposed model membrane and test method for microneedle insertion studies. *Int. J. Pharm.* 472, 65–73.
- Lau, S., Fei, J., Liu, H., Chen, W., Liu, R., 2017. Multilayered pyramidal dissolving microneedle patches with flexible pedestals for improving effective drug delivery. *J. Control. Release* 265, 113–119.
- Lee, J.W., Park, J.H., Prausnitz, M.R., 2008. Dissolving microneedles for transdermal drug delivery. *Biomaterials* 29, 2113–2124.
- Li, G., Badkar, A., Nema, S., Kolli, C.S., Banga, A.K., 2009. In vitro transdermal delivery of therapeutic antibodies using maltose microneedles. *Int. J. Pharm.* 368, 109–115.

- Liu, Y., Derby, B., 2019. Experimental study of the parameters for stable drop-on-demand inkjet performance. *Phys. Fluids* 31, 868.
- Luo, Z., Sun, W., Fang, J., Lee, K., Li, S., Gu, Z., Dokmeci, M.R., Khademhosseini, A., 2019. Biodegradable gelatin methacryloyl microneedles for transdermal drug delivery. *Adv. Healthc. Mater.* 8, e1801054.
- Ma, G., Wu, C., 2017. Microneedle, bio-microneedle and bio-inspired microneedle: A review. *J. Control. Release* 251, 11–23.
- Martanto, W., Davis, S.P., Holiday, N.R., Wang, J., Gill, H.S., Prausnitz, M.R., 2004. Transdermal delivery of insulin using microneedles in vivo. *Pharm. Res.* 21, 947–952.
- Martin, G.D., Hoath, S.D., Hutchings, I.M., 2008. Inkjet printing - the physics of manipulating liquid jets and drops. *J Phys: Conference Series* 105.
- Matadh, A.V., Jakka, D., Pragathi, S.G., Rangappa, S., Shivakumar, H.N., Maibach, H., Reena, N.M., Murthy, S.N., 2022. Polymer-coated polymeric (PCP) microneedles for controlled dermal delivery of 5-Fluorouracil. *AAPS PharmSciTech* 24, 9.
- Maurya, A., Nanjappa, S.H., Honnavar, S., Salwa, M., Murthy, S.N., 2018. Rapidly dissolving microneedle patches for transdermal iron replenishment therapy. *J. Pharm. Sci.* 107, 1642–1647.
- McAllister, D.V., Wang, P.M., Davis, S.P., Park, J.H., Canatella, P.J., Allen, M.G., Prausnitz, M.R., 2003. Microfabricated needles for transdermal delivery of macromolecules and nanoparticles: Fabrication methods and transport studies. *PNAS* 100, 13755–13760.
- McCrudden, M.T., Alkilani, A.Z., McCrudden, C.M., McAlister, E., McCarthy, H.O., Woolfson, A.D., Donnelly, R.F., 2014. Design and physicochemical characterisation of novel dissolving polymeric microneedle arrays for transdermal delivery of high dose, low molecular weight drugs. *J. Control. Release* 180, 71–80.
- Nasiri, M.I., Vora, L.K., Ershaid, J.A., Peng, K., Tekko, I.A., Donnelly, R.F., 2022. Nanoemulsion-based dissolving microneedle arrays for enhanced intradermal and transdermal delivery. *Drug Deliv. Transl. Res.* 12, 881–896.
- Nguyen, H.X., Banga, A.K., 2018. Delivery of methotrexate and characterization of skin treated by fabricated PLGA microneedles and fractional ablative laser. *Pharm. Res.* 35, 68.
- Palakurthi, N.K., Correa, Z.M., Augsburger, J.J., Banerjee, R.K., 2011. Toxicity of a biodegradable microneedle implant loaded with methotrexate as a sustained release device in normal rabbit eye: A pilot study. *J. Ocul. Pharmacol. Ther.* 27, 151–156.
- Panda, A., Shettar, A., Sharma, P.K., Repka, M.A., Murthy, S.N., 2021. Development of lysozyme loaded microneedles for dermal applications. *Int. J. Pharm.* 593, 120104.
- Paredes, A.J., Volpe-Zanutto, F., Permana, A.D., Murphy, A.J., Picco, C.J., Vora, L.K., Coulter, J.A., Donnelly, R.F., 2021. Novel tip-loaded dissolving and implantable microneedle array patches for sustained release of finasteride. *Int. J. Pharm.* 606, 120885.
- Peng, K., Vora, L.K., Tekko, I.A., Permana, A.D., Dominguez-Robles, J., Ramadan, D., Chambers, P., McCarthy, H.O., Larraneta, E., Donnelly, R.F., 2021. Dissolving microneedle patches loaded with amphotericin B microparticles for localised and sustained intradermal delivery: Potential for enhanced treatment of cutaneous fungal infections. *J. Control. Release* 339, 361–380.
- Permana, A.D., Anjani, Q.K., Sartini, Utomo, E., Volpe-Zanutto, F., Paredes, A.J., Evary, Y.M., Mardikasari, S.A., Pratama, M.R., Tuany, I.N., Donnelly, R.F., 2021. Selective delivery of silver nanoparticles for improved treatment of biofilm skin infection using bacteria-responsive microparticles loaded into dissolving microneedles. *Mater Sci Eng C Mater Biol Appl* 120, 111786.
- Pires, L.R., Amado, I.R., Gaspar, J., 2020. Dissolving microneedles for the delivery of peptides - Towards tolerance-inducing vaccines. *Int. J. Pharm.* 586, 119590.
- Quinn, H.L., Bonham, L., Hughes, C.M., Donnelly, R.F., 2015. Design of a dissolving microneedle platform for transdermal delivery of a fixed-dose combination of cardiovascular drugs. *J. Pharm. Sci.* 104, 3490–3500.
- Rojekar, S., Vora, L.K., Tekko, I.A., Volpe-Zanutto, F., McCarthy, H.O., Vavia, P.R., Donnelly, R.F., 2021. Etravirine-loaded dissolving microneedle arrays for long-acting delivery. *Eur. J. Pharm. Biopharm.* 165, 41–51.
- Scheuplein, R.J., Blank, I.H., 1971. Permeability of the skin. *Physiol. Rev.* 51, 702–747.
- Seong, K.Y., Seo, M.S., Hwang, D.Y., O’Cearbhaill, E.D., Sreenan, S., Karp, J.M., Yang, S. Y., 2017. A self-adherent, bullet-shaped microneedle patch for controlled transdermal delivery of insulin. *J. Control. Release* 265, 48–56.
- Singh, M., Haverinen, H.M., Dhagat, P., Jabbour, G.E., 2010. Inkjet printing-process and its applications. *Adv. Mater.* 22, 673–685.
- Tekko, I.A., Chen, G., Dominguez-Robles, J., Thakur, R.R.S., Hamdan, I.M.N., Vora, L., Larraneta, E., McElmoy, J.C., McCarthy, H.O., Rooney, M., Donnelly, R.F., 2020. Development and characterisation of novel poly (vinyl alcohol)/poly (vinyl pyrrolidone)-based hydrogel-forming microneedle arrays for enhanced and sustained transdermal delivery of methotrexate. *Int. J. Pharm.* 586, 119580.
- Thabet, Y., Lunter, D., Breitreutz, J., 2018. Continuous inkjet printing of enalapril maleate onto orodispersible film formulations. *Int. J. Pharm.* 546, 180–187.
- Thakral, S., Thakral, N.K., Majumdar, D.K., 2013. Eudragit: A technology evaluation. *Expert Opin. Drug Deliv.* 10, 131–149.
- Vander Straeten, A., Sarmadi, M., Daristotle, J.L., Kanelli, M., Tostanoski, L.H., Collins, J., Pardeshi, A., Han, J., Varshney, D., Eshaghi, B., Garcia, J., Forster, T.A., Li, G., Menon, N., Pyon, S.L., Zhang, L., Jacob-Dolan, C., Powers, O.C., Hall, K., Alsaiani, S.K., Wolf, M., Tibbitt, M.W., Farra, R., Barouch, D.H., Langer, R., Jaklenc, A., 2024. A microneedle vaccine printer for thermostable COVID-19 mRNA vaccines. *Nat. Biotechnol.* 42, 510–517.
- Verbaan, F.J., Bal, S.M., van den Berg, D.J., Groeninck, W.H., Verpoorten, H., Luttge, R., Bouwstra, J.A., 2007. Assembled microneedle arrays enhance the transport of compounds varying over a large range of molecular weight across human dermatomed skin. *J. Control. Release* 117, 238–245.
- Volpe-Zanutto, F., Ferreira, L.T., Permana, A.D., Kirkby, M., Paredes, A.J., Vora, L.K., A, P.B., Charlie-Silva, I., Raposo, C., Figueiredo, M.C., Sousa, I.M.O., Brisibe, A., Costa, F.T.M., Donnelly, R.F., Foglio, M.A., 2021. Artemether and lumefantrine dissolving microneedle patches with improved pharmacokinetic performance and antimalarial efficacy in mice infected with *Plasmodium yoelii*. *J. Control Release* 333, 298–315.
- Wang, P.M., Cornwell, M., Hill, J., Prausnitz, M.R., 2006. Precise microinjection into skin using hollow microneedles. *J. Invest. Dermatol.* 126, 1080–1087.
- Wiechers, J.W., 1989. The barrier function of the skin in relation to percutaneous absorption of drugs. *Pharm Weekbl Sci* 11, 185–198.
- Xing, M., Yang, G., Zhang, S., Gao, Y., 2021. Acid-base combination principles for preparation of anti-acne dissolving microneedles loaded with azelaic acid and matrine. *Eur. J. Pharm. Sci.* 165, 105935.
- Yang, G., He, M., Zhang, S., Wu, M., Gao, Y., 2018. An acryl resin-based swellable microneedles for controlled release intradermal delivery of granisetron. *Drug Dev. Ind. Pharm.* 44, 808–816.
- Zhao, L., Vora, L.K., Kelly, S.A., Li, L., Larraneta, E., McCarthy, H.O., Donnelly, R.F., 2023. Hydrogel-forming microarray patch mediated transdermal delivery of tetracycline hydrochloride. *J. Control. Release* 356, 196–204.